Spectroscopic Probe Analysis of Protein–Surfactant Interactions: The BSA/SDS System

Nicholas J. Turro and Xue-Gong Lei

Chemistry Department, Columbia University, New York, New York 10027

K. P. Ananthapadmanabhan* and M. Aronson

Unilever Research Center, Edgewater, New Jersey 07020

Received August 16, 1994. In Final Form: May 5, 1995®

The interactions and structure of complexes formed between bovine serum albumin (BSA) and the anionic surfactant sodium dodecyl sulfate has been investigated by spectroscopic probe techniques. Steady state and time-resolved fluorescence, electron spin resonance, and deuterium NMR spectroscopy have been employed as a multitechnique approach to investigate the structures which occur along the protein–surfactant isotherm. Three models of the protein–surfactant complex are considered. The results of the multitechnique approach are consistent with a structure which is predominantly of the "necklace and bead" type in which the unfolded protein wraps around surfactant micelles.

Introduction

Sodium dodecyl sulfate (SDS) is known to bind strongly to BSA (bovine serum albumin) and other proteins and cause their denaturation.[1–7] The denaturation is considered to be due to the surfactant-induced unfolding of the protein. In this context, the binding of SDS and other anionic surfactants to proteins has been studied extensively.[1–11] In fact, available literature[3,4,7] in this area shows that the binding isotherm of a ligand such as SDS onto a protein plotted as a function of equilibrium (free) ligand concentration typically displays four characteristic regions (Figure 1A), whose binding characteristics have been interpreted as follows. In the initial region (termed region a), at lowest concentrations of SDS, there exists some binding to specific high-energy sites on the protein. Region a is followed, in most cases, by either a plateau or a slow rising part of the isotherm (termed region b) and beyond it a third region (termed region c) corresponding to a massive increase in binding because of cooperative interactions. The unfolding of the protein is believed to occur in the cooperative binding region. Beyond the saturation point, the binding isotherm shows a plateau (termed region d), suggesting that further binding of the surfactant does not occur on the protein and that normal micelle formation occurs as excess surfactant is added. Under saturation binding conditions, 1 g of the protein can be expected to bind as much as 1.5–2 g of the surfactant.[2,8]

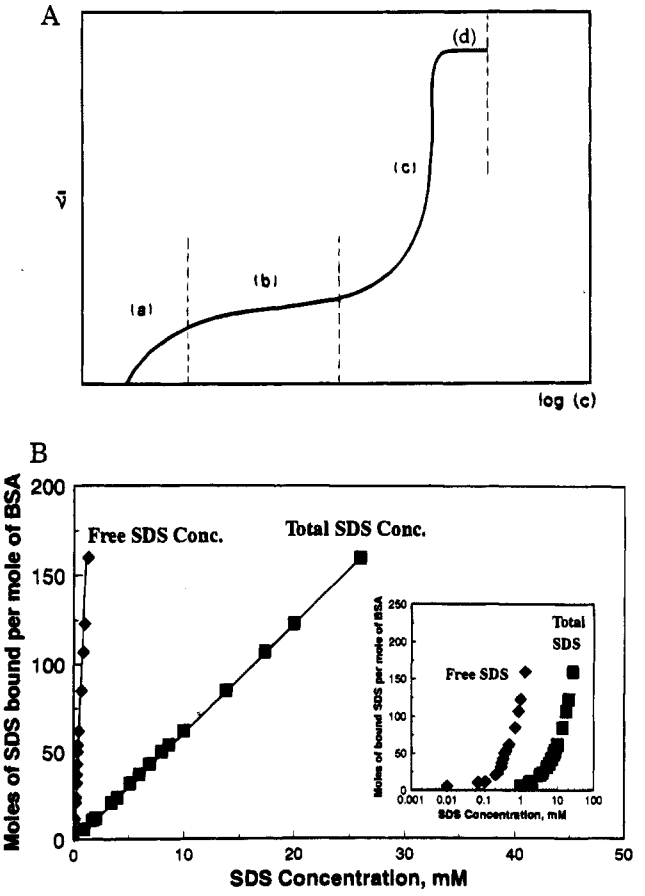

Figure 1. (A) Schematic plot of the number of bound ligands per protein molecule (ν) as a function of the logarithm of the free ligand concentration (c): region a, specific binding; region b, noncooperative binding; region c, cooperative binding; and region d, saturation. Reprinted with permission from ref 7. Copyright 1975 Portland Press. (B) Binding of SDS to BSA, replotted using the data given in ref 15. The curve labeled as free SDS shows the isotherm plotted as a function of equilibrium monomer SDS. The curve labeled as total SDS shows the isotherm as a function of total SDS (bound + free). Inset shows details at lower concentrations. pH 5.6, ionic strength 0.033 M buffer (0.024 M $NaH_2PO_4 \cdot 2H_2O$ and 0.0024 M Na_2HPO_4).

A typical binding isotherm of SDS to BSA (1%) replotted using the data given in ref 15 is shown in Figure 1B. Note

® Abstract published in *Advance ACS Abstracts,* June 15, 1995.

(1) Steinhardt, J.; Reynolds, J. A. *Multiple Equilibria in Proteins*; Academic Press: New York, 1969.
(2) Tanford, C. *The hydrophobic Effect: formation of micelles and biological membranes*, 2nd ed.; Wiley-Interscience: New York, 1980; Chapter 14.
(3) Schwuger, M. J.; Bartnik, F. G. In *Anionic Surfactants*; Gloxhuber, C., Ed.; Surfactant Science Series, Vol. 10; Marcel Dekker: New York, 1980; Chapter 1.
(4) Jones, M. N. *Chem. Soc. Rev.* **1992**, *21*, 127.
(5) Robb, I. D. In *Anionic Surfactants, Physical Chemistry of Surfactant Action*; Lucassen-Reyenders, Ed.; Surfactant Science Series, Vol. 10; Marcel Dekker: New York, 1981; p 109.
(6) Ananthapadmanabhan, K. P. In *Interactions of surfactants with polymers and proteins*; Goddard, E. D., Ananthapadmanabhan, K. P., Eds.; CRC Press: Boca Raton, 1993; p 319.
(7) Jones, M. N. *Biochem. J.* **1975**, *151*, 109.
(8) Reynolds, J. A.; Tanford, C. *Proc. Natl. Acad. Sci. U.S.A.* **1970**, *66* (3), 1002.
(9) Yang, J. T.; Foster, J. F. *J. Am. Chem. Soc.* **1943**, *75*, 5560.
(10) Goddard, E. D.; Pethica, B. A. *J. Chem. Soc.* **1953**, 2659.
(11) Decker, R. V.; Foster, J. F. *Biochemistry* **1966**, *5* (4), 1242.

0743-7463/95/2411-2525$09.00/0

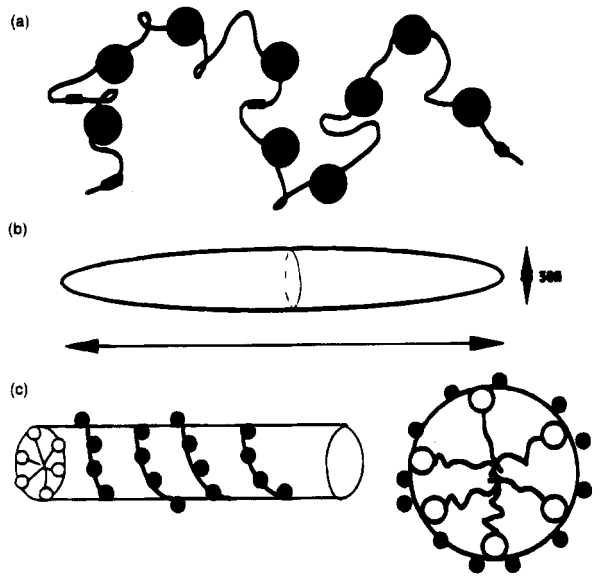

Figure 2. Proposed structure of protein–surfactant complexes; see ref 18.

that here the isotherm is plotted as a function of both the equilibrium and total SDS concentration. The total includes both the bound and the unbound SDS. Interestingly, even at the lowest equilibrium concentration of 0.01 mM SDS, there appears to be binding to six sites on the protein, indicating that the initial high-energy binding region (region a) is at a still lower concentration. However, regions b and c can be seen clearly in this isotherm. Note that region c when plotted as a function of total SDS extends over a wide concentration region, in this case, as high as 30 mM. The almost vertical nature of the isotherm in region c (curve for free SDS) indicates that almost all of the added SDS binds cooperatively to the protein. Interestingly, in the tested region, there appears to be as much as (160 molecules of SDS)/(molecule of BSA), and this corresponds to about (0.7 g of SDS)/(g of BSA). Since the data did not extend to the plateau region, the saturation binding of SDS to BSA is not evident from this figure. According to Reynolds and Tanford,[2,8] the saturation binding of SDS to BSA is as high as (1.4 g of SDS)/(g of BSA).

Even though classical binding characteristics of SDS to BSA and other proteins has been established and the binding phenomenon itself is used in the commonly employed SDS–polyacrylamide gel electrophoresis, the microstructure of protein–surfactant complexes is not well understood. Information concerning the structure of protein–surfactant complexes has come from rheological,[12,13] spectroscopic,[14,15] electrophoretic,[16] binding,[2,4,7] and scattering studies.[17,18] From these considerable investigations have emerged three useful models for the structure of SDS–protein complexes involved in protein denaturation (Figure 2): (a) a correlated "necklace and bead" model in which a cluster of micelle-like structures are stabilized by the protein;[16–18] (b) a "rod-like" prolate ellipsoidal surfactant aggregate with a semiminor axis around 18 Å, corresponding to that of the surfactant chain length[2,12] with the protein wrapping around the aggregate; and (c) a "flexible capped helical cylindrical micelle" with the proteins wrapping around the micelle.[19] Recently, a SANS (small angle neutron scattering) study of BSA[17,18] and OVA (ovalbumin) complexes with SDS led to the conclusion that the necklace and bead structure of protein surfactant aggregates accounted for the scattering behavior of the system. In fact, the scattering data allow the determination of the size of individual micelles bound to the protein under various conditions.[17,18]

Although several studies suggest significant changes in protein structure along the binding isotherm of the surfactant, no studies have been carried out utilizing a combination of molecular spectroscopic probes to elucidate the microstructure of the surfactant–protein complex. We felt that the multitechnique spectroscopic probe approach would provide a range of information and would be appropriate for the analysis of complex problems as protein binding and unfolding. Fluorescence,[20–26] ESR,[27,28] and NMR[29,30] techniques involve convenient and readily available measurements which provide simple spectral parameters that can be related to the microstructure of surfactant aggregates such as micelles and polymer–surfactant complexes.[20–30] For example, the type of information which can be obtained using various molecular probes and spectroscopic techniques is given in Table 1. The specific information on the structure of the protein–surfactant complex that can be inferred from the spectroscopic probe measurements is given in Table 2.

For example, the fluorescence and ESR probes can report differences in polarity as well as microviscosity of their environment and should be able to provide information on the mechanism of uncoiling of the protein itself and on the changes in the structure of protein–surfactant complexes at different levels of surfactant binding. Furthermore, information on the size of surfactant aggregates can be obtained from measurements of steady state and time-resolved excimer formation. Determination of the relative sizes of the aggregates should help differentiate between the three types of structures proposed for the surfactant–protein aggregates mentioned above. For example, the prolate ellipsoidal structure and the cylindrical structure should yield relatively large aggregation numbers compared to the necklace and bead structure. The NMR probes, on the other hand, can provide information on the mobility of different parts of the surfactant molecule, e.g., head group region versus tails, and in turn, provide information on the location of the protein in relation to the surfactant head groups and the tails in the complex. For example, the NMR technique

(12) Reynolds, J. A.; Tanford, C. *J. Biol. Chem.* **1970**, *245* (19), 5161.
(13) Rao, P. F.; Yakagi, T. *J. Biochem.* **1989**, *106*, 365.
(14) Laurie, O.; Oakes, J. *J. Chem. Soc., Faraday Trans. 1* **1975**, 1324.
(15) Oakes, J. *J. Chem. Soc., Faraday Trans. 1* **1974**, *70*, 2200.
(16) Shirahama, K.; Tsujii, K.; Takagi, T. *J. Biochem.* **1974**, *75*, 309.
(17) Chen, S. H.; Teixeira, J. *Phys. Rev. Lett.* **1986**, *57* (20), 2583.
(18) Guo, X. H.; Zhao, N. M.; Chen, S. H.; Texeira, J. *Biopolymers* **1990**, *29*, 335.
(19) Lundahl, P.; Greijer, E.; Sandberg, M.; Cardell, S.; Eriksson, K. O. *Biochem. Biophys. Acta* **1986**, *873*, 20.
(20) Turro, N. J.; Yekta, A. *J. Am. Chem. Soc.* **1978**, *100* (18), 5951.
(21) Zana, R. In *Surfactant solutions*; Zana, R., Ed.; Surfactant Science Series, Vol. 22; Marcel Dekker: New York, 1987; p 241.
(22) Atik, S. S.; Nam, M.; Singer, C. A. *Chem. Phys. Lett.* **1979**, *67*, 75.
(23) Turro, N. J.; Tanimoto, Y. *Photochem. Photobiol.* **1981**, *34*, 173.
(24) Zana, R.; Yiu, S.; Stsrazielle, C.; Lianos, P. *J. Collid Interface Sci.* **1981**, *80*, 208.
(25) Kalyanasundaram, K.; Thomas, J. K. *J. Am. Chem. Soc.* **1977**, *99*, 2039.
(26) Thomas, J. K. *Chem. Rev.* **1980**, *80* (4), 283.
(27) Witte, F. M.; Buwalda, P.; Engberts, J. F. N. *Colloid Polym. Sci.* **1987**, *265*, 42.
(28) Taupin, C.; Dvolaitzky, M. In *Surfactant Solutions*; Zana, R., Ed.; Surfactant Science Series, Vol. 22; Marcel Dekker: New York, 1987; p 359.
(29) Lindman, B.; Soderman, O.; Wennerstrom, H. In *Surfactant Solutions*; Zana, R., Ed.; Surfactant Science Series; Vol. 22; Marcel Dekker: New York, 1987; p 295. Also: Taupin, C.; Dvolaitzky, M. *Ibid.*, p 359.
(30) Cabane, B. *J. Phys. Chem.* **1977**, *81*, 179, 1639.

Table 1. List of Molecular Probes and Measured Parameters

probe	technique	observable	exptl param	microscopic params
pyrene	fluorescence monomer (steady state)	$I(\lambda)$	I_3/I_1	ϵ_μ, polarity
pyrene	fluorescence excimer (steady state)	$I(\lambda)$	I_e/I_m	η_μ, N, microviscosity, rel size
pyrene	fluorescence (time resolved)	$I(t)$	τ	N, K_{diff}, aggregation no.
TNS	fluorescence (steady state)	$I(\lambda)$	I and λ_{max}	ϵ_μ, polarity
5-doxylstearic acid	ESR	$I(\mathbf{H})$	a, $\Delta\omega$	ϵ_μ, τ_{rot}, polarity, microviscosity
$CH_3(CH_2)_{10}CD_2OSO_3Na$	^2H FT-NMR	$I(\mathbf{H})$	a, $\Delta H_{1/2}$	η_μ, mobility of head group
$CD_3(CD_2)_{10}CD_2OSO_3Na$	^2H FT-NMR	$I(\mathbf{H})$	a, $\Delta H_{1/2}$	η_μ, mobility of head group and surfactant tail

Table 2. Microstructural Features of Protein–Surfactant Complex Revealed by Various Molecular Probes

probe and technique	macroscopic param	aspect of protein–surfactant complex reported
pyrene/TNS steady state fluorescence	polarity	surfactant-induced protein uncoiling; TNS competes with SDS for cationic sites on the protein and does not get solubilized in SDS micelles; can report competition effects
pyrene excimer formation	microviscosity, rel size of surfactant aggregate	rel size of surfactant aggregates, microviscosity of aggregates; can distinguish necklace and bead structure from the prolate ellipsoid and the cylindrical micelle
pyrene, time-resolved fluorescence	size of surfactant aggregate	surfactant aggregate size in the protein–surfactant complex; can distinguish the necklace and bead structure from the ellipsoidal and cylindrical micelle-type structures
5-doxylstearic acid, ESR	polarity, microviscosity	protein uncoiling, microviscosity
$CH_3(CH_2)_{10}C^2H_2OSO_3Na$, ^2H NMR	mobility of head group of surfactant	location of head groups in relation to the protein
$C^2H_2(C^2H_2)_{10}C^2H_2OSO_3Na$, ^2H NMR	mobility of head group, tails, and chains	location of head groups and tails in relation to the protein

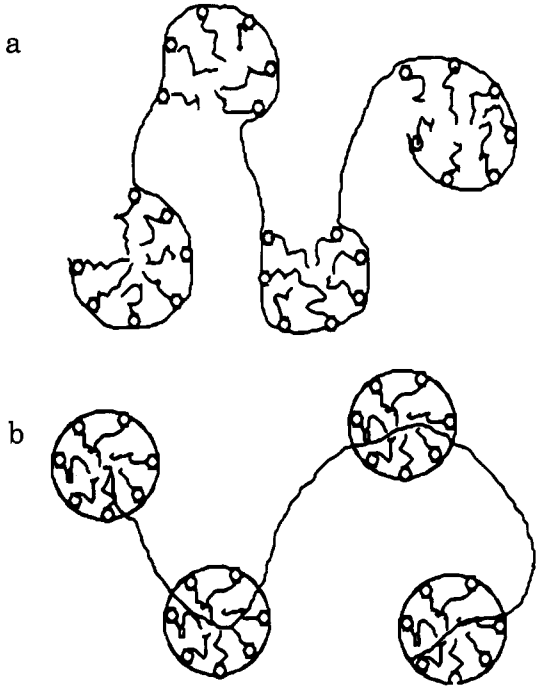

Figure 3. Two possible "necklace and bead structures" of protein–surfactant complexes: (a) the protein wraps around the micelles, and the mobility of the surfactant head group is decreased; (b) the micelles nucleate on the protein hydrophobic sites, and the mobility of the surfactant head groups is not affected.

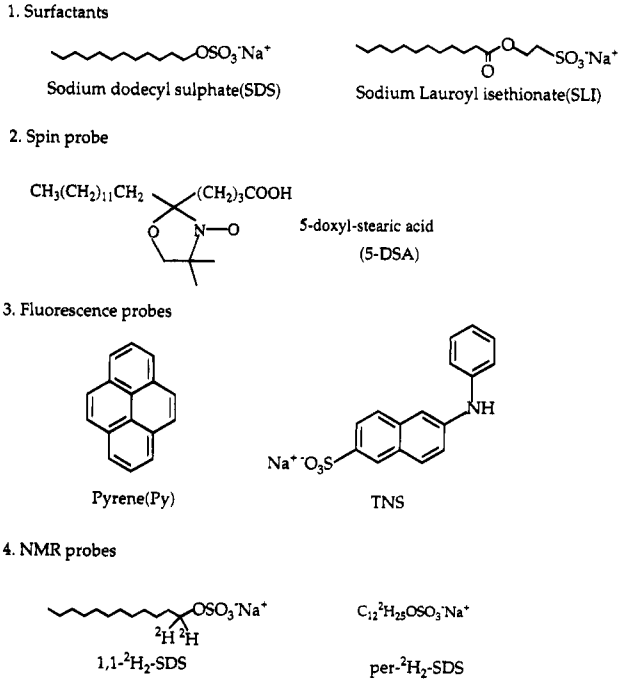

Figure 4. Probes.

can distinguish between the two possible structures, one in which the surfactant aggregate wraps around the hydrophobic sites because of hydrophobic interactions versus the one in which the protein wraps around the surfactant head groups (Figure 3).

In this investigation, fluorescence, ESR, and NMR probes are used to characterize the interaction of sodium dodecyl sulfate (SDS) with a model water-soluble protein, bovine serum albumin (BSA).

Experimental Section

Materials. High-purity SDS purchased from Fluka Chemials was used without further purification. Pyrene and 5-doxylstearic acid were purchased from Aldrich Chemical Co., and TNS (2-*p*-toluidinylnaphthalenesulfonate) was purchased from Molecular Probes Inc. Perdeuterated SDS and [1,1-$^2H_2$]SDS were purchased from Cambridge Isotopes, Inc. The structures of various probes used in the study are given in Figure 4.

Methods. Static fluorescence was measured using a Perkin-Elmer fluorescence spectrophotometer (Model MPF-6). ESR spectra were recorded using a Bruker spectrophotometer (Model ESP 300). NMR spectra were obtained using a Bruker instrument (Model AF 250 mHz). Dynamic fluorescence measurements were performed using a single photon counting device.[23] The

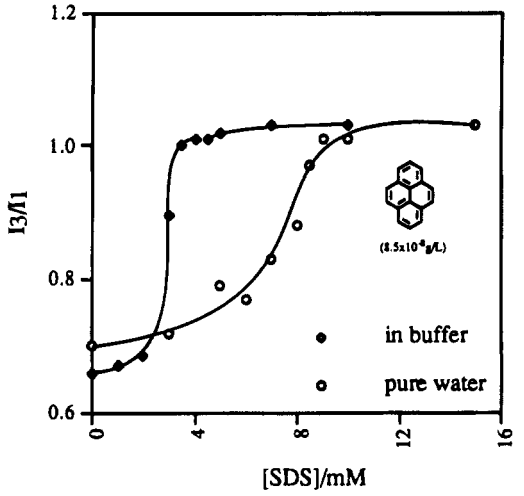

Figure 5. I_3/I_1 ratios of pyrene as a function of concentration of SDS in water and in buffer (0.0243 mol dm^{-3} $KH_2PO_4 \cdot 2H_2O$, 0.00243 mol dm^{-3} K_2HPH_4, 0.033 mol dm^{-3} ionic strength at pH 5.6) at 35 °C.

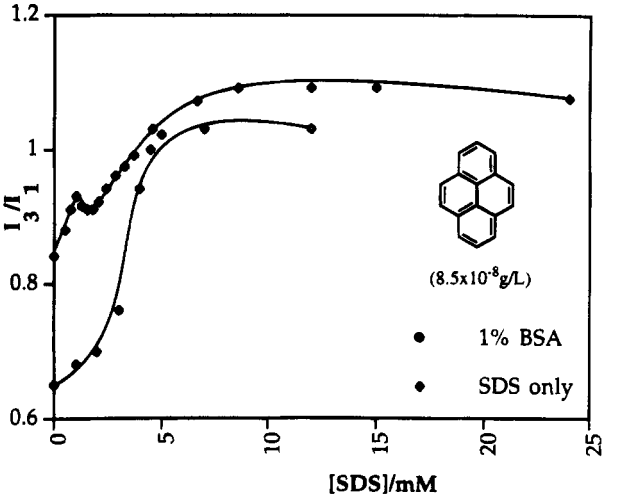

Figure 6. I_3/I_1 ratio of pyrene in the presence and absence of 1% BSA as a function of total SDS concentration in 0.2 M buffer.

latter data was analyzed to obtain the size of surfactant aggregates.[21,24]

In most of the experiments, the BSA concentration was maintained at the level of 1% and the surfactant concentration was varied from about 1 mM to about 200 mM. The solutions were prepared containing phosphate (0.024 mol/L KH_2PO_4, 0.002 43 mol/L K_2HPO_4, pH 5.6) or acetate (0.1 mol/L NaOAc–HOAc, pH = 5.1) buffers. Unless otherwise stated, the probes were dissolved at the desired levels in BSA solutions.

Results and Discussion

Steady State Fluorescence Studies. *Pyrene Monomer Fluorescence.* The ratio of the third to the first fluorescence band of pyrene monomer (I_3/I_1) is a well-established parameter which reflects the polarity experienced by the pyrene probe.[21,25] A low value reflects a more polar environment than a high value. The observed values typically range from ca. 0.6 for water as a solvent to 1.4 for a hydrocarbon as solvent. The cmc value for SDS can be determined by measurement of I_3/I_1 of pyrene in protein-free solutions (Figure 5) as a check of the technique. In agreement with the literature,[25] the intensity ratio I_3/I_1 has a value of 0.65 in water and 1.0–1.1 in SDS micelles. The cmc determined from the data in Figure 5 for SDS is 8.6 mM, in agreement with the reported values.[25] Analogous measurements in a buffer system show the cmc of SDS to be 3.3 mM (Figure 5).

The I_3/I_1 values for pyrene plotted as a function of total SDS in the presence and absence of 1% BSA are shown in Figure 6. As can be seen, the intensity ratio has a value of 0.84 even in the absence of any surfactant. The pyrene, in this case, indicates a polarity which is in between that which the pyrene reports for water and for surfactant micelles. The probe technique clearly shows that pyrene is solubilized in the hydrophobic regions of the protein. Addition of surfactant changes the I_3/I_1 values, indicating that the surfactant is interacting with BSA. The results in Figure 6 suggest an increase in hydrophobicity followed by a small, but definite reduction and then a sharp increase beyond a certain concentration of surfactant. The values of I_3/I_1 at very high concentrations of surfactant are around 1.0, similar to those reported earlier for micellar solutions. *Thus, these experiments suggest that the hydrophobicity of the regions in which the probe is dissolved varies as the isotherm is traversed.*

Pyrene Excimer Formation. Pyrene monomer fluorescence measurements are usually performed at probe concentrations corresponding to the pyrene saturation in water (less than 10^{-6} M). In aqueous solutions containing surfactants and other molecules which have hydrophobic environments, pyrene solubility can be increased. In such systems, when the solution is excited under appropriate conditions, pyrene molecules in the excited state can interact with a ground state pyrene to form an excimer, which displays a characteristic broad-band fluorescence which occurs at longer wavelengths than for the monomer.[21,26] The ratio of the fluorescence intensity of the excimer to monomer (I_e/I_m) is a parameter which can be taken as a measure of the relative amounts of excimer to monomer in the system, which in turn provides information on the distribution of probes in the aggregates present in the system and on the "microviscosity" of the system.[26]

Table 3. Pyrene Excimer Formation in SDS–BSA Solutions

system	I_3/I_1	I_e/I_m	comments
SDS 35 mM (1%)	1.03	0.52	
SDS 35 mM (1%) in buffer	1.16	1.29	buffer increases micelle size; more pyrene per micelle; higher I_e/I_m
SDS 35 mM (1%) + BSA (1%) in buffer	1.12	0.47	lower I_e/I_m than in BSA-free solutions indicating smaller micelle size

[a] Pyrene concentration = 0.37 mM.

In general, at fixed levels of the surfactant and pyrene, the larger the micelle size, the lower the number of micelles and, therefore, the more pyrene per micelle. Such a situation results in higher I_e/I_m values and provides information on the relative size of micelles. I_e/I_m values for the BSA–SDS system are shown in Table 3. Clearly, in the absence of BSA, an increase in the size of micelles is inferred from the increase in the I_e/I_m. In the presence of BSA (1%) in buffer solutions, the I_e/I_m values drop significantly, suggesting that the size of protein-bound micelles is smaller than the corresponding free micelles; i.e., for a particular concentration of the surfactant, there are more micelles. Note that free micelles are not expected under these conditions because the level of total SDS in the system is only 35 mM. On the basis of the information in Figure 1B, 35 mM SDS is either just about that required to saturate the BSA or still somewhere in the rising part of the isotherm. If we assume that 1.4 g of SDS is required to saturate BSA, the 35 mM SDS is positively in the rising part of the isotherm. Therefore, the size of micelles inferred from the I_e/I_m data of pyrene corresponds to protein-bound SDS aggregates. Furthermore, the values of I_e/I_m suggest that the size of micelles in BSA solutions

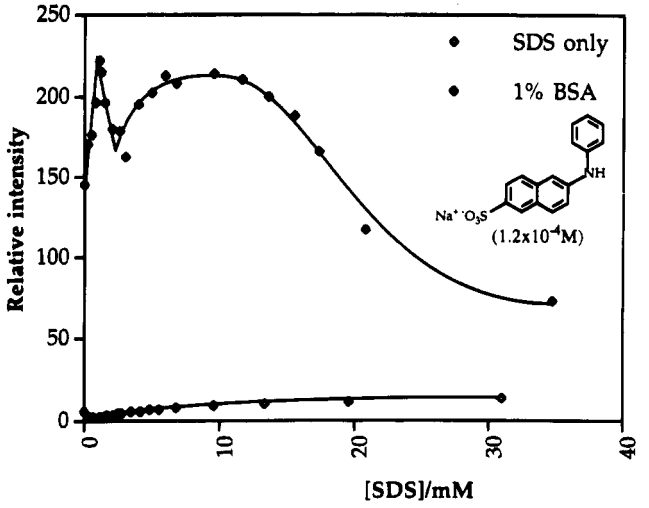

Figure 7. Fluorescence intensity of TNS (1.25×10^{-6} M) in the presence and absence of 1% BSA as a function of total SDS concentration.

under these conditions is about the same as the size of free micelles in water, i.e., unbuffered solutions. *These observations suggest that the micelle-like aggregates formed on the protein are smaller than the corresponding micelles formed in protein-free solutions.*

TNS Steady State Fluorescence. Because pyrene is neutral and hydrophobic, it is solubilized in SDS micelles and does not compete with SDS for binding to cationic sites on the protein. The fluorescence measurements have been performed also with another probe, TNS, which is hydrophilic and possesses an anionic sulfonate group and therefore can compete with SDS for cationic sites on the protein. TNS, however, does not have any affinity for the SDS micelles.[31] As a probe, TNS has very low fluorescence intensity in a highly polar solvent such as water, but the yield of fluorescence increases dramatically with increasing hydrophobicity of the surrounding environment.[31] Fluorescence characteristics of TNS in the presence and absence of 1% BSA are given in Figure 7. In agreement with the literature results,[31] TNS exhibits low intensity in BSA-free SDS solutions, indicating that it does not partition into anionic micelles. The high fluorescence yield of the spectrum for the SDS–BSA system shows that TNS in the absence of the surfactant senses a hydrophobic region. Importantly, in the presence of BSA and SDS, with surfactant addition, the hydrophobicity first increases and then decreases. This is followed by a sharp increase and another reduction. The behavior of TNS is similar to that of pyrene (Figure 6) in the first three regions, and it differs from that of pyrene only at high concentrations, where pyrene reports a micelle-like environment and the TNS a more polar environment.

The initial increase in the hydrophobicity of both the probes can be attributed to the cobinding of the surfactant and the probe molecules near the hydrophobic regions of the protein. The reduction in the hydrophobicity indicates the release of some of the probe molecules into a more hydrophilic phase because of competition for binding with the surfactant. As would be expected, the competition is more clearly seen with TNS than pyrene. Beyond the minimum, the probes report an increase in the hydrophobicity, and this reversal occurs at total SDS levels of 2.4 and 2.7 mM respectively for pyrene and TNS. Interestingly, these correspond closely to the onset of a sharp rise in the binding isotherm (Figure 1B), indicating that in this region massive binding of the surfactant begins

(31) Niu, S.; Gopidas, K. R.; Turro, N. J. *Langmuir* **1992**, *8*, 1271.

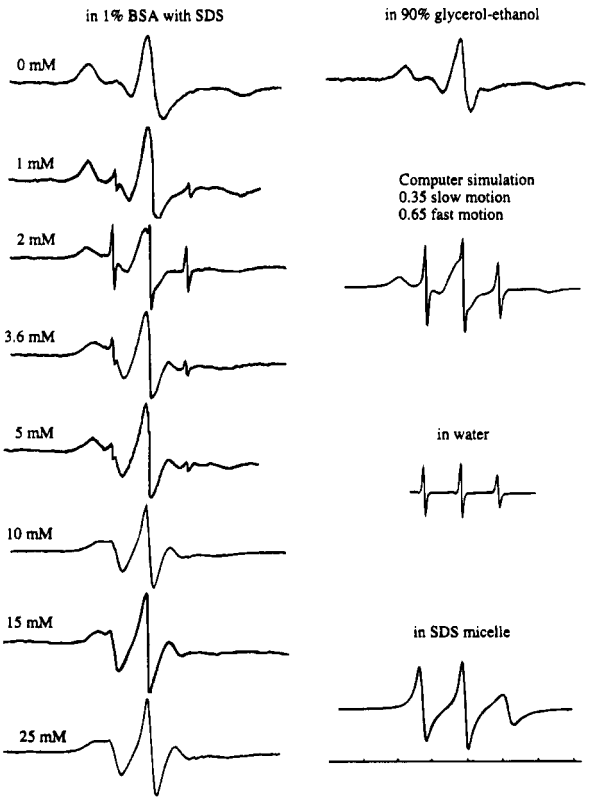

Figure 8. ESR spectra of 5-doxylstearic acid (1×10^{-4} M) in 1% BSA solution as a function of total SDS concentration. Also included are some of the controls.

to occur on the protein, leading to its uncoiling. As the protein opens up, the number of available sites, especially hydrophobic sites, should increase markedly. Thus, it is suggested that the increase in the hydrophobicity in this region of the isotherm is due to the binding of the probes and the surfactant to the hydrophobic regions made available by the protein unfolding. Here, while pyrene may be solubilized in the SDS–protein aggregate, TNS may be competing with the surfactant for the protein sites. At higher surfactant concentrations, SDS begins to displace the protein-bound TNS and, therefore, the probe is expelled into the aqueous phase. Thus, the observation that the TNS spectrum continues to change even at the highest level of SDS (total 35 mM) indicates that this concentration is in cooperative binding region c of the binding isotherm and that BSA-free micelles do not form under these conditions. Pyrene, on the other hand, remains as a part of the hydrophobic SDS aggregates bound to the protein, and the polarity of these aggregates appears to be similar to that of SDS micelles formed in protein-free solutions.

Thus, the changes in the fluorescence characteristics of pyrene and TNS clearly indicate the surfactant-induced uncoiling of the protein and support the formation of micelle-like aggregates at high concentrations of SDS.

ESR Measurements. ESR spectra of 5-doxylstearic acid (5-DSA) show a typical nitroxide sharp three-line spectrum characteristic of "unrestricted motion" of the probe in water and a modified, broadened three-line spectrum characteristic of "restricted mobility" in micellar solutions (Figure 8). Although information on the mobility of the probe is readily available at the qualitative level by simple inspection of the nitroxide ESR spectra, a more quantitative analysis allows computation of the ESR parameters of hyperfine coupling constants and correlation times, from which the polarity and "microviscosity" of the probe environment, respectively, can be deduced. The

5-DSA spectrum in surfactant-free BSA solutions and at low levels of surfactant appears to be similar to its spectrum in a concentrated glycerol–ethanol solution having a viscosity of 250 cP. Thus, in BSA, the probe is present in a relatively viscous environment of the protein. The probe, being amphiphilic, may be acting like SDS at such low levels and may be binding by both ionic and hydrophobic interactions. Interestingly, as the total SDS concentration is increased to 1 and 2 mM levels, some of the probe molecules sense a water-like environment with very low viscosity (sharp three-signal feature in Figure 8). In this region, a fraction of the probe is displaced by the surfactant into more mobile and more polar regions. These are consistent with the fluorescence data for pyrene and TNS which show their displacement into more polar regions. At 3.6 mM SDS, however, the displaced probe appears to be solubilized again in a hydrophobic region of intermediate mobility. This result is also consistent with the speculation deduced from fluorescence probe measurements; i.e., in this region the surfactant-induced uncoiling of the protein results in more hydrophobic sites for the binding of both the surfactant and the probe. With an increase in SDS concentration, the spectrum appears to become progressively more similar to that in BSA-free micellar SDS solutions, suggesting that the aggregates formed on BSA are similar to micelles. It can, however, be seen that even at the highest level tested (25 mM SDS) the probe motion is more restricted in the presence of BSA than in the absence of it, indicating that 25 mM still corresponds to region c in the isotherm.

It is clear from the above results that *both fluorescence and ESR probes report initial binding of the surfactant possibly by ionic and hydrophobic interactions, followed by the displacement of the probe.* The probes also report the surfactant-induced uncoiling of the BSA. The surfactant aggregates in this region appear to be similar to surfactant micelles. This picture of surfactant binding to proteins is consistent with the available information in the literature.[14–18]

Size of Surfactant Aggregates from Pyrene Excimer Decay Measurements. The steady state fluorescence measurements with pyrene and TNS as the probes are consistent with a model of the formation of micelle-like aggregates on the backbone of the protein. This is also in agreement with the necklace and bead model for protein–surfactant complexes.[14–18] If such aggregates exist, measurements of their size should be possible through measurements of the time-correlated fluorescence of pyrene. Time-resolved fluorescence[21–24] was employed to estimate the size of surfactant aggregates formed on BSA. The experimental conditions were kept similar to those reported for SANS measurements[17,18] so that the fluorescence results could be compared to SANS results. The SDS concentrations corresponded to levels in the cooperative binding region and, in some cases, possibly beyond that required for saturation binding.

The pyrene fluorescence decay measurements involve the determination of the decay of the pyrene fluorescence under conditions of simultaneous monomer decay and excimer decay. The overall decay behavior is then analyzed using eq 1[22] for fluorescence decay in a fragmented medium to determine n, the average number of pyrenes per aggregate,

$$I_m(t) = I_m(0) \exp\{-k_0 t + n(\exp(-k_e t)-1)\} \quad (1)$$

where $I_m(0)$ and $I_m(t)$ are monomer fluorescence at time 0 and time t and k_0 and k_e are the rate constants for monomer and excimer formation. At large values of t, the eq 1 reduces to the form of eq 2. Equation 3 represents an alternate form to handle the data.

$$I_m(t) = I_m(0) \exp[-k_0 t - n\} \quad (2)$$

$$\ln\{I_m(0)/I_m(t)\} = k_0 t + n \quad (3)$$

Thus, at very large values of t, the slopes of $\ln\{I_m(0)/I_m(t)\}$ vs t should be equal to k_0 and the intercept should be n, i.e., the average number of pyrene molecules per aggregate. Importantly, the above plot for various concentrations of pyrene should yield the same slope at very large values of t, corresponding to the value of k_0. This is clearly a check for the validity of the assumptions in the kinetic model, especially whether or not the aggregate is behaving like a fragmented medium.

The absolute aggregation number can be estimated from the value of n. If c_P is the concentration of pyrene in solution, C is the total surfactant concentration, and C_{agg} is the SDS concentration at which aggregation begins on the protein, then the aggregation number, N, is related to pyrene concentration by the relation[21,24]

$$c_P = n\{(C - C_{agg})/N\} \quad (4)$$

Since all of the terms in eq 4 except N are known, the aggregation number can be calculated.

For a particular concentration of SDS in BSA solution, several concentrations of pyrene were used to generate a series of decay curves. The curves were then fitted to the double exponential equation 1 using a computer program provided by Professor F. C. DeSchryver of the University of Leuven, Belgium, to obtain values of k_0, k_e, and n. The results obtained showed that, for given concentrations of BSA and SDS, the values of k_0 were essentially constant for different concentrations of pyrene, indicating that the assumption of fragmented medium is correct. The absolute value of the aggregation number estimated using the above equations shows the size of the aggregates in the protein–surfactant complexes to be smaller than that of conventional micelles under the same conditions (Table 4). Note that the SDS levels used for lifetime measurements range from 17 to 105 mM. Interestingly, both the lifetime and the aggregation number appear to change much more in the 17–52 mM region than in the 70–105 mM region, possibly suggesting that the formation of free micelles occurs at levels above about 52 mM SDS. This is consistent with the expected saturation binding of 1.4 g of SDS to 1 g of BSA[2,8] in the sense that only at a concentration of about 49 mM (1.4%) SDS will there be enough SDS in the system to attain the minimum amount to saturate the protein. Since there will be some free SDS in equilibrium with the bound SDS, the actual total SDS

Table 4. Aggregation Number[a] of SDS and Lifetime of Pyrene as a Function of Total [SDS] in 1% BSA Buffer[b]

	0.6 M buffer			0.2 M buffer		
	this expt			this expt		
[SDS]/mM	N	τ (ns)	N_{SANS}[c]	N	τ (ns)	N_{SANS}[c]
17	33	211		29	223	
26				49	201	
35	43	179	29	52	187	38
43	53	167		67	182	
52			43	70	175	43
70	75	140	42	74	172	42
105	82	142	39	82	166	50

[a] For 35 mM (1%) SDS in 0.6 M buffer alone, the aggregation number is 106 (35 °C); fluorescence lifetime is 136. [b] 0.5 M NaCl + 0.1 M NaOAc–HOAc, pH = 6.1 at 35 °C, or 0.1 M NaCl + 0.1 M NaOAc–HOAc at 25 °C. [c] From ref 18. Data for LDS (lithium dodecyl sulfate) in buffer solution.

concentration required to saturate 1% BSA will be higher than 49 mM. Thus, the observed increase in the aggregate size in the 17–52 mM range can be attributed to a real increase in the size of protein-bound micelles rather than an average size of free and protein-bound micelles. In this region, the measured size of protein–SDS aggregates appears to be less than that of the corresponding protein-free micelles. The smaller size of protein-bound micelles is consistent with the results reported for polymer-bound micelles in such systems as PEO–SDS and PAA–TTAB (polyacrylic acid–tetradecyltrimethylammonium bromide) systems.[30,32-35] *The absolute values of aggregation numbers clearly support the necklace and bead structure of the protein–surfactant complex, since the other two, namely, the prolate ellipsoid and the cylindrical micelles, should have yielded much larger aggregation numbers.*

As mentioned above, at 70 and 105 mM SDS, free micelles may coexist with the protein-bound micelles. If this is indeed the case, analysis of fluorescence decay curves will have to be done taking into account the partitioning of pyrene into protein-bound and protein-free micelles. Since this was not done in the present study, the aggregation numbers indicated in Table 4 at SDS levels above 70 mM are average values of protein-bound and regular micelles. Another possibility is that the protein-bound micelles evolve from its small size, for example from an aggregation number of 29 at 17 mM SDS (0.2 M ionic strength) to an average of about 70–80 where both the free micelles and the protein-bound micelles coexist. It is not clear whether under these conditions there are two populations of micelles with distinctly different average aggregation numbers. Obviously, as the protein to surfactant ratio decreases in the system, the micelles should resemble the conventional micelles. Thus, the initial micelles formed will be predominantly stabilized by the protein at high protein to surfactant ratios and eventually become similar to conventional micelles at low protein to surfactant ratios with the structures stabilized predominantly by the counterions. The above two possibilities, namely, two populations of micelles vs micelles that are stabilized by both the proteins and counterions at some stage of the evolutionary process, depending upon the ratio of protein to surfactant in the system, cannot be distinguished by the aggregation numbers and the lifetime measurements.

The values of aggregation numbers reported[17,18] for LDS (lithium dodecyl sulfate)–BSA system determined using the SANS technique are also given in Table 4. It is clear that the fluorescence results provide aggregation numbers which are of the same order of magnitude, but consistently smaller than those provided by the SANS measurements. The differences in the absolute numbers may result from differences in the counterion in the system, namely, Li versus Na. It is known, for example, that Na binds more strongly to alkyl sulfate micelles than Li,[36,37] consistent with smaller micelle size for the latter.[38] The important point is that *both techniques indicate the formation of a micelle-like aggregate in the presence of the protein.* Thus, the necklace and bead structure of protein–surfactant complexes[16,18] is well supported by the present study.

The above measurements provide support for the ability of fluorescence methods to provide reliable aggregation numbers for protein-bound micelles and provide an alternative method to the more difficult and less accessible SANS measurements.

NMR Studies. The spectroscopic probe techniques presented above support a model in which surfactant aggregates form on the unfolded protein backbone. However, the structure of the aggregate, i.e., whether the protein wraps around the micelle or the micelle nucleates on the protein (Figure 3), is not clearly established. In the case of charged polymer–oppositely charged surfactant systems, the energetics of electrostatic interactions would favor a structure where the polymer wraps around the aggregate. This, however, need not be true for a protein–surfactant aggregate, especially if the protein opens up, as surfactant binds, to expose more hydrophobic regions. In the latter case, the surfactant aggregate can condense around the hydrophobic regions of the protein. This would imply a protein–surfactant structure in which the protein does not wrap around the aggregate, but actually goes through the center of it (Figure 3). *If the protein actually wraps around the micelle (Figure 3a), then the mobility of the head group region will be markedly hindered. Micelles nucleating on the protein (Figure 3b), however, will not influence the head group mobility significantly, but may affect the surfactant chains and tails to a greater extent.* Such changes in the motion of different segments of the surfactant molecules can be monitored using NMR techniques. Chemical shifts, band width, and spin lattice relaxation parameters can provide useful information on the structure and dynamics of the surfactant–protein complex and assist in differentiating between the two models of Figure 3. However, since proton NMR of the BSA–SDS system was too complex to make meaningful interpretations, ^2H NMR studies of deuterated SDS were conducted.

The NMR studies employed two deuterated surfactants (Figure 4). The ^2H NMR spectra of [1,1-$^2H_2$]SDS with ^2H labeling only near the head group show two peaks, one corresponding to water labeled with ^2H and the other to the C^2H_2 group next to the head group of the surfactant (Figures 9–11). The results for [1,1-$^2H_2$]SDS in Figure 10 show that as the concentration is increased from premicellar (7 mM [1,1-$^2H_2$]SDS) to micellar levels (35 mM [1,1-$^2H_2$]SDS), some broadening occurs, indicating the restricted mobility of that region of the surfactant as a result of aggregation. Addition of 0.2 M buffer to the 35 mM [1,1-$^2H_2$]SDS also has a measurable effect on head group mobility. Importantly, in the presence of the protein, the broadening is increased markedly, *indicating a significant reduction in the head group mobility and the involvement of the head group in the protein–surfactant aggregate, consistent with the model depicted in Figure 3a, in which the protein wraps around the micelles.*

The ^2H NMR of perdeuterated SDS shows four resolved peaks in addition to the water peak (Figures 9–11). Two of these correspond to the two C^2H_2 groups closest to the head group (at 4.02 and 1.6 ppm). The other two signals correspond to the end C^2H_2 group farthest from the head group (0.8 ppm) and the rest of the alkyl chain (1.2 ppm). Thus, in the presence of BSA, the tail group continues to show some mobility, but the head group region is broadened significantly. This, along with the data reported above, strongly suggests that the protein interacts significantly with the head group of the surfactant aggregate. *Thus, the NMR study provides further support*

(32) Kiefer, J.; Soamsundaran, P.; Ananthapadmanabhan, K. P. *Proc. of the P & G UERP Symp. on Polymer Solutions, Blends and Interfaces*; Noda, I., Rubingh, D. N., Eds.; Elsevier: Amsterdam, 1992; p 423.
(33) Mukerjee, P.; Mysels, K. J.; Kapauan, P. *J. Phys. Chem.* **1967**, *71*, 4166.
(34) Aronson, M.; Princen, H. *Colloids Surf.* **1982**, *4*, 173.
(35) Lindman, B.; Thalberg, K. In *Interactions of Surfactants with Polymers and Proteins*; Goddard, E. D., Ananthapadmanabhan, K. P., Eds.; CRC Press: Boca Raton, 1993; p 203.
(36) Mukerjee, P.; Mysels, K. J.; Kapauan, P. *J. Phys. Chem.* **1967**, *71*, 4166.
(37) Aronson, M.; Princen, H. Colloids Surf. **1982**, *4*, 173.
(38) Lindman, B. In *Surfactants*; Tadros, Th. F., Ed.; Academic Press: New York, 1983, p 83.

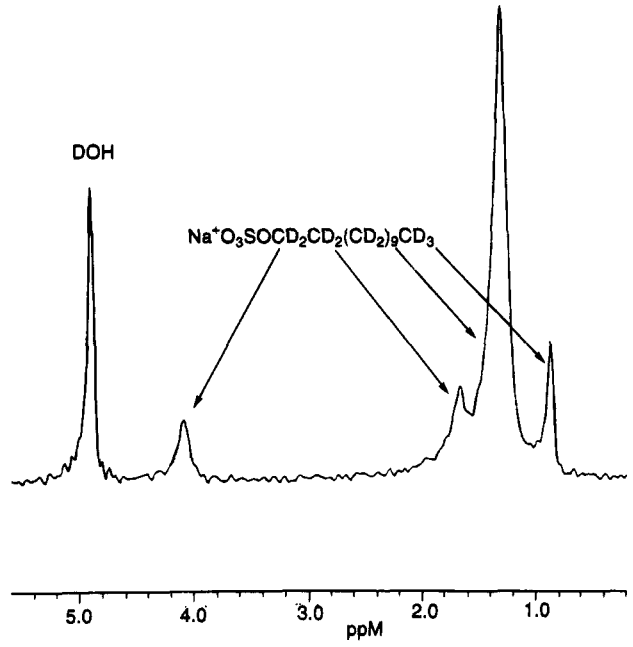

Figure 9. ^2H NMR spectrum of 6 mM perdeuterated SDS in water.

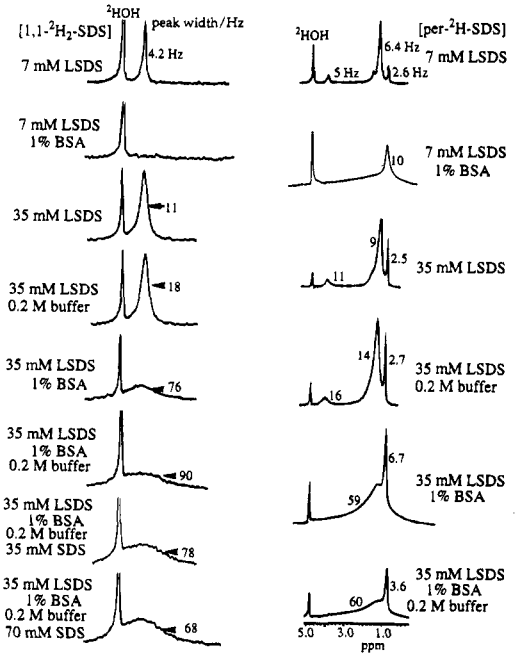

Figure 10. ^2H NMR spectra of [1,1-$^2H_2$]SDS (left) and perdeuterated SDS (right) in various solutions. Concentrations of the labeled SDS are shown as LSDS, while concentrations of unlabeled SDS are indicated by SDS.

for a structure of the protein–surfactant aggregate in which the protein actually wraps around the micelle (Figure 3a).

NMR tests were conducted not only in the cooperative binding region where protein unfolding occurs (region c in Figure 1) but also at SDS levels where saturation binding of SDS to BSA is expected. For example, the last two spectra in Figure 10 correspond to systems having 35 mM [1,1-$^2H_2$]SDS and 35 or 70 mM unlabeled SDS. Thus, their total concentrations of SDS are 70 and 105 mM, respectively. In this region, the formation of free micelles should lead to an increased mobility of the head groups. The spectra for 70 and 105 mM total SDS in Figure 11 do not show much change in the head group mobility, and this is possibly because of the relatively low concentration of the labeled molecule in this system. However, the

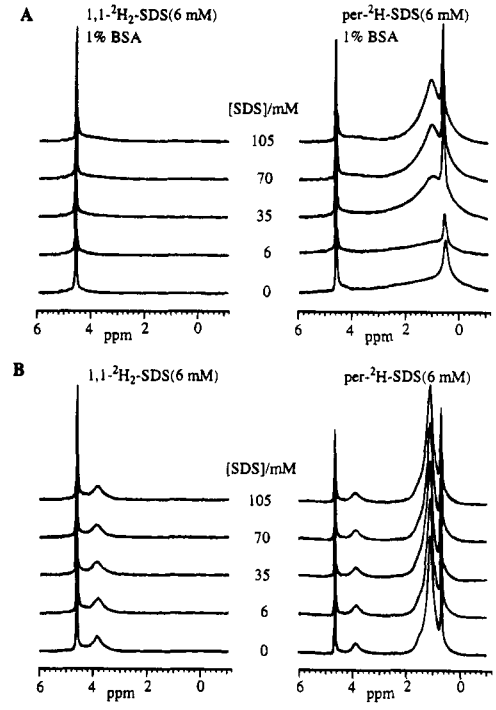

Figure 11. SDS effect on the ^2H NMR spectra of deuterated SDS solution in the presence (A) or absence (B) of 1% BSA (0.2 M ionic strength). The concentration of the labeled SDS is 6 mM; concentrations of unlabeled SDS are shown in the middle.

results obtained using higher levels of labeled SDS given in Figure 10 show some narrowing of the head group region compared to that at 35 mM, indicating the presence of free micelles. This is also consistent with the pyrene lifetime and aggregation number results, which also suggested the presence of protein-free micelles at concentrations above about 70 mM. As discussed earlier in the excimer decay section, the evolution of aggregates with low aggregation numbers at high protein to surfactant ratios (<35 mM) to those with a larger average size at low protein to surfactant ratios (>70 mM) rather than the existence of two populations of micelles cannot be ruled out from these measurements. The results of the present NMR and fluorescence decay measurements cannot distinguish between the above two situations unequivocally since both can account for the narrowing of the head group region and relatively small changes in lifetime and aggregation number at 70 and 105 mM SDS.

Summary and Conclusions

Fluorescence, ESR, and ^2H NMR spectroscopy have provided valuable information on the SDS-induced uncoiling of BSA and the structure of the resultant protein–surfactant complex in aqueous solutions. Figure 12 summarizes the results. At low SDS concentrations (region a in the isotherm, Figure 12a), the surfactant molecules bind specifically through ionic and perhaps hydrophobic interactions to the protein. This binding causes the protein to expand somewhat and allows noncooperative binding (region b in the isotherm, not shown in Figure 12). Then there is an abrupt cooperative binding and formation of the necklace and bead structures as the unfolding protein opens sites which induce micelle formation and the protein wraps around the micelles (Figure 12c). There appears to be some growth in the protein-bound micelles (Figure 12d). It is not clear as to where exactly free micelles in equilibrium with protein-bound micelles begin to form in the system. It is also not clear whether, under such conditions, there are two

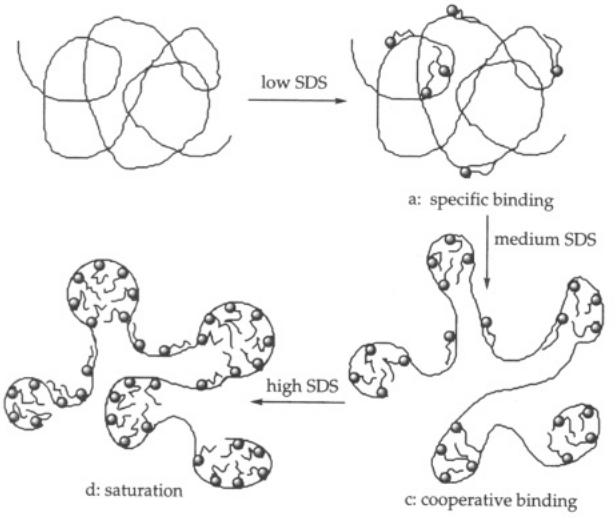

Figure 12. Surfactant-induced protein unfolding.

populations of micelles with distinctly different aggregation numbers. The possibility of a gradual transition from a predominantly protein stabilized micelle at high protein to surfactant ratios to micelles that are similar to conventional micelles stabilized predominantly by counterions can also account for the system behavior.

Some of the specific conclusions are as follows:

1. Fluorescence and ESR probes clearly show the surfactant-induced uncoiling of BSA in aqueous solutions. In the denatured region, the protein promotes the formation of micelle-like aggregates by wrapping around them and thereby presumably lowering the electrostatic field. The probes display several unusual transitions as a function of the protein–surfactant ratios in the system.

2. Dynamic fluorescence shows the size of surfactant aggregates on BSA to be smaller than that of normal SDS micelles. The actual size is somewhat larger than that reported from SANS for lithium dodecyl sulfate,[17,18] but the difference may reflect the different counterions used. The results support the necklace and bead structure of protein–surfactant aggregates.

3. Analysis of the NMR spectra of the two deuterated SDS probes indicates that the BSA is predominantly coiled around the exterior of the bound SDS micelles.

LA9406416